

Buckling of Steel Cylindrical Shells with an Elliptical Cutout

Mahmoud Shariati and Masoud Mahdizadeh Rokhi*

Department of Mechanical Engineering, Shahrood University of Technology, Shahrood, Iran.

Abstract

Numerical simulation and analysis of steel cylindrical shells with various diameter and length having an elliptical cutout, subjected to axial compression were systematically carried out in this paper. The investigation examined the influence of the cutout size, cutout angle and the shell aspect ratios L/D and D/t on the pre-buckling, buckling, and post-buckling responses of the cylindrical shells. For several specimens, an experimental investigation was also carried out via an INSTRON 8802 servo hydraulic machine and the results obtained from the experiments were compared with numerical results. A very good accordance was observed between the results obtained from the finite element simulation and the experiments. Furthermore, some equations in the form of a buckling load reduction factor were developed.

Keywords: cylindrical shells, elliptical cutout, buckling, FEM, experimental analysis

1. Introduction

Cylindrical shells are frequently used in the manufacturing of aircrafts, missiles, boilers, pipelines, automobiles, and some submarine structures. These structures may experience axial compression loads in their longevity and buckle through these loads. Furthermore, these structures usually have disruptions, such as cutouts, which may have destroyer effects on their stability.

The problem of buckling in cylindrical shells has been a preoccupation of researchers for more than a century. At first, researchers focused on the determination of the buckling load in the linear elastic zone, but experimental studies (Arbocz, 1991; Jullien and Limam, 1998) showed that the buckling capacity of thin cylindrical shells is much lower than the amount determined in the classic theories (Timoshenko, 1961).

Almorth *et al.* (1973) performed a complex nonlinear analysis for cylindrical shells with two opposite circular cutouts subject to axial compression. Starnes (1974) performed another experimental and numerical study on the buckling effect of circular, square, and rectangular cutouts in cylindrical shells subject to axial compression. Toda (1983) performed an experimental investigation on the cylindrical shells with circular holes subject to axial

compression. Furthermore, he placed ring-shaped stiffeners around the cutout and studied the effect of stiffeners on the buckling of cylindrical shells with circular cutouts. Jullien and Limam (1998) studied the effect of square, rectangular, and circular cutouts on the buckling of cylindrical shells subject to axial compression, and developed a parametrical formula for the shape and dimensions of the cutouts. The influences of the position and number of cutouts were also studied. The software program used for the finite element method was CASTEM2000. At the same time, Yeh *et al.* (1999) analytically and experimentally studied the bending and buckling of moderately thick-walled cylindrical shells with cutouts.

Lim *et al.* (2003) studied the elastic buckling of vertical cylindrical shells under combined end pressure and body force. They presented the total potential energy functional based on the Goldenveizer-Novozhilov thin shell theory and solved the buckling problem using the Ritz method. In their study the effects of the shell thickness and length on buckling parameter were investigated.

Together with the employing of thin-walled structures in civil engineering, numerous researches on thin-walled structural members have been extensively investigated. In the past, most research activities focused on the analysis of behaviour of thin-walled members, which are made of isotropic material such as steel, zincalume-metal and aluminium and did not take into account the orthotropic or anisotropic materials (Kuwamura, 2003; Camotim *et al.*, 2005; Nadia *et al.*, 2005; Rasmussen *et al.*, 2005).

Tafreshi (2002) numerically studied the buckling and post-buckling response of composite cylindrical shells subjected to internal pressure and axial compression loads

Note.-Discussion open until November 1, 2010. This manuscript for this paper was submitted for review and possible publication on February 14, 2010; approved on June 15, 2010.

*Corresponding author
Tel: +989153082813
E-mail: masoud_mahdizadeh@yahoo.com

using ABAQUS. She studied the influences of size and orientation of cutouts and found that an increase of internal pressure resulted in an increase in buckling capacity. Also, Tafreshi and Colin (2006) performed a numerical study using non-linear finite element analysis to investigate the response of composite cylindrical shells subjected to combined load, in which the post buckling analysis of cylinders with geometric imperfections is carried out to study the effect of imperfection amplitude on critical buckling load.

Poursaeidi *et al.* (2004) considered an elastoplastic material and used ABAQUS Software to analyze the plastic behavior of cylindrical shells with cutouts under pure bending. The shell had a circular cross section and both ends had been clamped. The shape of the cutouts in the shells was circular or rectangular. The influence of the size, location and number of the cutouts on the limiting bending moment of a cylindrical shell was presented. Vartdal *et al.* (2005) studied on simply supported steel tubes with rectangular cutouts of different sizes positioned at their mid-length subjected to axial compression to assess the effect of the cutouts on the deformation behavior. Han *et al.* (2006) studied the effect of dimension and position of square-shaped cutouts in thin and moderately thick-walled cylindrical shells of various lengths by nonlinear numerical methods using the ANSYS software. They also compared their results with experimental studies on moderately thick-walled shells. Finally, they developed several parametric relationships based on the analytical and experimental results using the least squares regression method. Shariati and Mahdizadeh (2008) studied the effect of position of elliptical cutouts with identical dimensions on the buckling and post-buckling behavior of cylindrical shells with different diameters and lengths and developed several parametric relationships based on the Numerical and experimental results using the Lagrangian polynomial method. Also, Shariati and Mahdizadeh (2009) performed a similar numerical study using ABAQUS software to investigate the response of steel cylindrical shells with different lengths and diameters, including elliptical cutout subjected to bending moment. They presented some relations for finding of buckling moment of these structures.

Various researchers studied how the buckling strength of thin cylindrical shell structures are influenced by the presence of local geometrical imperfections such as axisymmetric cosine shaped dimple imperfections (Amazigo and Budiansky, 1972), diamond shaped dimple imperfections (Krishnakumar and Forster, 1991), axisymmetric concave and convex ring shaped imperfections (Schneider, 2006), weld induced axisymmetric imperfections (for e.g. Pircher and Bridge, 2001; Pircher *et al.*, 2001). Also, Schenk and Schuëller (2007) have investigated the effect of random geometric imperfections on the critical load of isotropic, thin-walled, cylindrical shells under axial compression with rectangular cutouts. The individual and combined effects of random boundary and geometric

imperfections on the limit loads of such cylindrical shells were also treated in their study.

Prabu *et al.* (2010) studied the effect of variation of size and angle of inclination of dents on buckling strength of the short carbon steel cylindrical shell by FE modeling of cylindrical shell with single dent having different size and angles of inclination at half of the height of the cylindrical shell. Blachut (2010) computed the load bearing capacity of axially compressed mild steel cylinders with non-uniform axial length. He assumed that the initial geometric imperfection had a sinusoidal shape along the compressed edge.

In this paper, a set of linear and nonlinear analyses using the ABAQUS finite element software were carried out to study the effect of cutout size and cutout angle on the buckling and post-buckling behavior of cylindrical shells with different diameters and lengths, as follows: $(L/D_1)=2.857, 6.5, 10$; $(D_1/t)=53.846$; and $(L/D_2)=2.495, 5.676, 8.732$; $(D_2/t)=61.667$. Where (L/D) and (D/t) are length to diameter and diameter to thickness ratios of cylindrical shells, respectively. Additionally, several buckling tests were performed using an INSTRON 8802 servo hydraulic machine, and the results were compared with the results of the finite element method. Very good accordance between the results obtained from experiments and numerical simulations was observed. Finally, based on the experimental and numerical results, formulas are presented for the computation of the buckling load in such structures.

2. Numerical Analysis Using the Finite Element Method

The numerical simulations were carried out using the general finite element program ABAQUS 6.4-PR11.

2.1. Geometry and mechanical properties

In this study, cylindrical shells with three different lengths ($L=120$ mm, 273 mm, 420 mm), and two different diameters ($D=42$ mm, 48.1 mm) were analyzed. An elliptical geometry was selected for cutouts that were created in the specimens. Furthermore, the thickness of shells was $t=0.78$ mm. Fig. 1 shows the geometry of specimens and elliptical cutouts. In Fig. 1, parameter a shows the size of the cutout along the longitudinal axis of the cylinder, parameter b shows the size of the cutout in circumferential direction of the cylinder, and θ is the angle between the greater diameter of the ellipse and the section plane of the cylinder. The distance between the center of the cutout and the lower edge of the shell is designated by L_0 .

Specimens were nominated as follows $D42-L120-L_060-a-b-\theta$; where the numbers following D and L show the diameter and length of the specimen, respectively. Also, the number following L_0 shows distance between the center of the cutout and the lower edge of the shell. For cutouts with an angle of 0° , the number for the angle

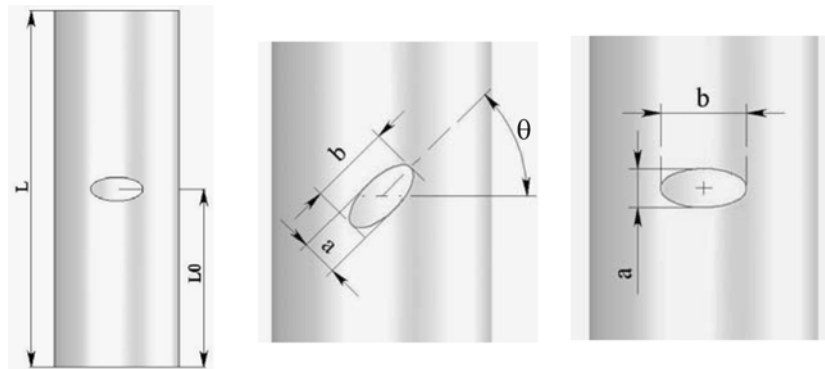


Figure 1. Geometry of specimens and cutouts.

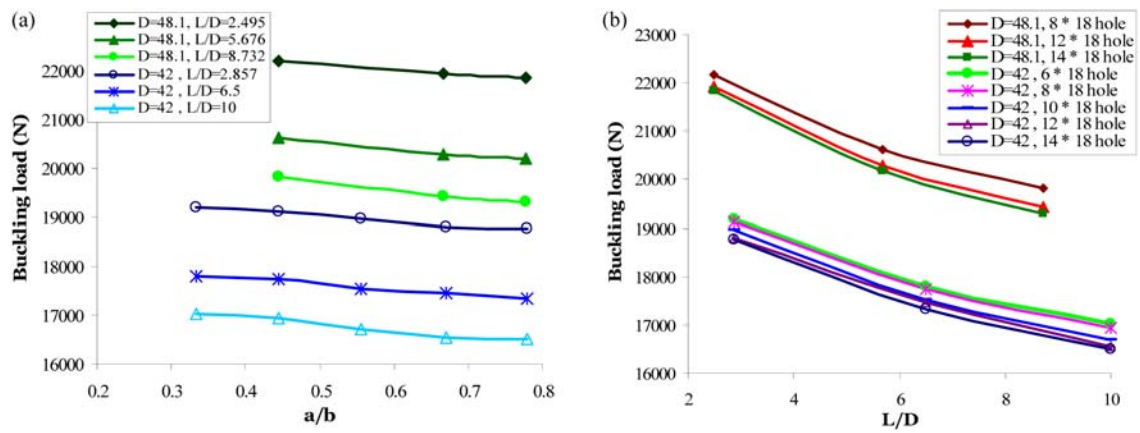


Figure 2. Summary of the buckling capacity of cylindrical shells versus (a) ratio a/b and (b) L/D , for elliptical cutout with constant width and various heights.

is not included in the specimen designation.

The cylindrical shells used for this study were made of mild steel alloy. The mechanical properties of this steel alloy were determined according to ASTM E8 standard (ASTM A 370-05, 2005), using the INSTRON 8802 servo hydraulic machine. The stress-strain and stress-plastic strain curves can be found in paper of Shariati and Mahdizadeh (2008). The value of elasticity module was computed as $E=187.73$ GPa and the value of yield stress was obtained as $\sigma_y=212$ MPa. Furthermore, the value of Poisson ratio was assumed $\nu=0.3$.

2.2. Boundary conditions

In this study, the cylindrical shells were considered as clamped. For applying boundary conditions on the edges of the cylindrical shells, two rigid plates were used that were attached to the ends of the cylinder.

In order to analyze the buckling subject to axial load similar to what was done in the experiments; a 10-mm displacement was applied centrally to the center of the upper plate, which resulted in a distributed, compressive load on both edges of the cylinder. Additionally, all degrees of freedom in both the lower plate and the upper plate, except in the direction of longitudinal axis, were constrained.

2.3. Selection of element type and size

The nonlinear element S8R5 which is an eight-node element with five degrees of freedom per node (ABAQUS user manual) was used in analyses.

Starting with a $6\text{ mm} \times 6\text{ mm}$ element size, using the nonlinear buckling analysis, a convergence study was conducted for a thin cylindrical shell (specimen D42-L420-L₀210-7.9-17.92-90). The results obtained from each refinement stage of the mesh were compared with previous stage and were summarized in Table 1.

Presented results in Table 1 show that buckling load value converges to about 18500 N. Also, the accuracy of all results is good. In order to shun time consuming analyses, an element size equal to $3\text{ mm} \times 3\text{ mm}$ was considered as general element size in the remaining numerical analyses. For this element size, the average aspect ratio of all elements is 1.34 which is adequate. The analyses showed that a typical element size of 0.3 mm could be used to model the area around the cutout.

2.4. Analytical process

To analyze the buckling of cylindrical shells, two analysis methods, Linear eigenvalue analysis and geometric nonlinear, were employed using the "Buckle" and "Static-Riks" solvers respectively. For more information about

Table 1. Mesh convergence study of the cylindrical shells

Approximate Element size (mm×mm)	Buckling load (N)	Average max. angle (Deg.)	Average min. angle (Deg.)	Average aspect ratio	Number of elements	Difference percent with respect to previous value
6×6	18520.1	94.17	85.75	2.04	2884	-----
5×5	18549.9	93.08	86.86	1.97	3908	0.161
4×4	18529.1	92.35	87.61	1.66	5132	-0.112
3×3	18513.6	91.49	88.48	1.34	8060	-0.084
2.7×2.7	18510.1	91.34	88.64	1.28	9008	-0.019
2.5×2.5	18507.4	91.15	88.83	1.22	10468	-0.014

Table 2. Summary of numerical analysis for cylindrical shells including an elliptical cutout with constant width and various heights

Model designation	Shell length (mm)	Cutout size (a×b)	Buckling Load (N)
D42-L420-Perfect	420	-----	22792.8
D42-L420-L ₀ 210-6-17.95	420	6×17.95	17030.8
D42-L420-L ₀ 210-8-17.7	420	8×17.7	16938.7
D42-L420-L ₀ 210-10-17.95	420	10×17.95	16701.9
D42-L420-L ₀ 210-12.05-17.95	420	12.05×17.95	16540.1
D42-L420-L ₀ 210-14.05-17.95	420	14.05×17.95	16500.2
D42-L273-Perfect	273	-----	22814.8
D42-L273-L ₀ 136.5-6-18	273	6×18	17793.7
D42-L273-L ₀ 136.5-8-17.68	273	8×17.68	17746.4
D42-L273-L ₀ 136.5-10-18	273	10×18	17533.9
D42-L273-L ₀ 136.5-12-17.8	273	12×17.8	17459.7
D42-L273-L ₀ 136.5-14.08-18	273	14.08×18	17332.2
D42-L120-Perfect	120	-----	22751.6
D42-L120-L ₀ 60-6-18	120	6×18	19179.6
D42-L120-L ₀ 60-8-17.6	120	8×17.6	19120.4
D42-L120-L ₀ 60-10-18	120	10×18	18967.5
D42-L120-L ₀ 60-12.1-18	120	12.1×18	18782
D42-L120-L ₀ 60-14.05-18	120	14.05×18	18772.1
D48.1-L420-Perfect	420	-----	25876.9
D48.1-L420-L ₀ 210-7.94-17.54	420	7.94×17.54	19828.4
D48.1-L420-L ₀ 210-12-18	420	12×18	19432.9
D48.1-L420-L ₀ 210-14-18	420	14×18	19302.4
D48.1-L273-Perfect	273	-----	25858.7
D48.1-L273-L ₀ 136.5-8.02-17.86	273	8.02×17.86	20623.2
D48.1-L273-L ₀ 136.5-12-18	273	12×18	20276.7
D48.1-L273-L ₀ 136.5-14-18	273	14×18	20184.1
D48.1-L120-Perfect	120	-----	25825.4
D48.1-L120-L ₀ 60-8.04-17.75	120	8.04×17.75	22177.3
D48.1-L120-L ₀ 60-12-18	120	12×18	21918.6
D48.1-L120-L ₀ 60-14-18	120	14×18	21836.4

these FE analyses you can refer to Shariati and mahdizadeh (2008), Lee *et al.* (2009) and ABAQUS user manual.

2.5. Reference cylindrical shell

Generally, it is preferable to use dimensionless data for plotting the curves. In the present study, for making the buckling load dimensionless, the ‘reference buckling load’ of the shell was defined to be as eq. (1):

$$N_{ref} = t \times \sigma_Y \tag{1}$$

In eq. (1), N_{ref} is the reference load, which is, in fact, the compressive load necessary for yielding of the perfect cylindrical shell per unit of the shell section perimeter. t is the thickness of the shells, and σ_Y is the yield stress of the material used in the making of shells. Therefore, the reference load of the specimens is calculated as eq. (2):

$$N_{ref} = 0.78 \text{ mm} \times 212 \text{ N/mm}^2 = 165.36 \text{ N/mm} \tag{2}$$

Also, the amount of compressive deformation of the shells was made dimensionless using the length of the shells.

3. Results of Numerical Analysis

In this section, the results of the buckling analyses of cylindrical shells with elliptical cutouts of different sizes and angles, using the finite element method, are presented. Three different shell lengths were analyzed, representing short ($L=120$ mm), intermediate-length ($L=273$ mm) and long cylindrical shells ($L=420$ mm).

3.1. The effects of cutout size, L/D and D/t ratios

3.1.1. Analysis of the effect of change in cutout height on the buckling load

To study the effect of a change in cutout height on the buckling load of cylindrical shells, cutouts with constant width (18 mm) were created in the mid-height position of shells. Then, with changing the height of the cutouts from

6 to 14 mm, the change in buckling load was studied. The results of the analysis are shown in Table 2. Furthermore, buckling load vs. a/b and L/D ratios curves produced from the FEM, are shown in Figs. 2a and 2b, respectively.

Figure 2a shows that with increasing cutout height, the buckling load decreases. But the amount of reduction in the buckling load is slight. The reduction in the buckling load with the increase of cutout height from 6 mm to 14 mm for long, intermediate-length, and short shells with a diameter of 42 mm was about 3, 2.6, and 2.1%, respectively. For shells with a diameter of 48.1 mm, with the increase of cutout height from 6 mm to 14 mm, the buckling load decreases 2.6, 2.1, and 1.5% for long, intermediate-length, and short shells, respectively. Therefore, it can be seen that longer and slender shells are more sensitive to the effects of change in cutout height, even though these variations are slight. It is also evident from Fig. 2b that shells with larger diameters and identical cutouts are more resistant to buckling.

Table 3. Summary of numerical analysis for cylindrical shells including an elliptical cutout with constant height and various widths

Model designation	Shell length (mm)	Cutout size (a×b)	Buckling Load (N)
D42-L420-Perfect	420	-----	22792.8
D42-L420-L ₀ 210-8-9.98	420	8×9.98	18654.3
D42-L420-L ₀ 210-8-12	420	8×12	18146.6
D42-L420-L ₀ 210-8-14.05	420	8×14.05	17691.1
D42-L420-L ₀ 210-8-16	420	8×16	17270.9
D42-L420-L ₀ 210-8-17.7	420	8×17.7	16938.7
D42-L273-Perfect	273	-----	22814.8
D42-L273-L ₀ 136.5-8-9.95	273	8×9.95	19224.3
D42-L273-L ₀ 136.5-8-12	273	8×12	18775.3
D42-L273-L ₀ 136.5-7.96-13.84	273	7.96×13.84	18406.7
D42-L273-L ₀ 136.5-8-16	273	8×16	18028.9
D42-L273-L ₀ 136.5-8-17.68	273	8×17.68	17746.4
D42-L120-Perfect	120	-----	22751.6
D42-L120-L ₀ 60-8-10.88	120	8×10.88	20241.7
D42-L120-L ₀ 60-8-12	120	8×12	19949.7
D42-L120-L ₀ 60-8.27-14.07	120	8.27×14.07	19691.7
D42-L120-L ₀ 60-8-16	120	8×16	19343.2
D42-L120-L ₀ 60-8-17.6	120	8×17.6	19120.4
D48.1-L420-Perfect	420	-----	25876.9
D48.1-L420-L ₀ 210-7.95-9.88	420	7.95×9.98	21550.2
D48.1-L420-L ₀ 210-7.96-13.84	420	7.96×13.84	20644.5
D48.1-L420-L ₀ 210-7.94-17.54	420	7.94×17.54	19828.4
D48.1-L273-Perfect	273	-----	25858.7
D48.1-L273-L ₀ 136.5-8.02-9.92	273	8.02×9.92	22104.3
D48.1-L273-L ₀ 136.5-8.02-13.92	273	8.02×13.92	21293.2
D48.1-L273-L ₀ 136.5-8.02-17.86	273	8.02×17.86	20623.2
D48.1-L120-Perfect	120	-----	25825.4
D48.1-L120-L ₀ 60-8-9.9	120	8×9.9	23512.5
D48.1-L120-L ₀ 60-8.04-13.85	120	8.04×13.85	22824.9
D48.1-L120-L ₀ 60-8.04-17.75	120	8.04×17.75	22177.3

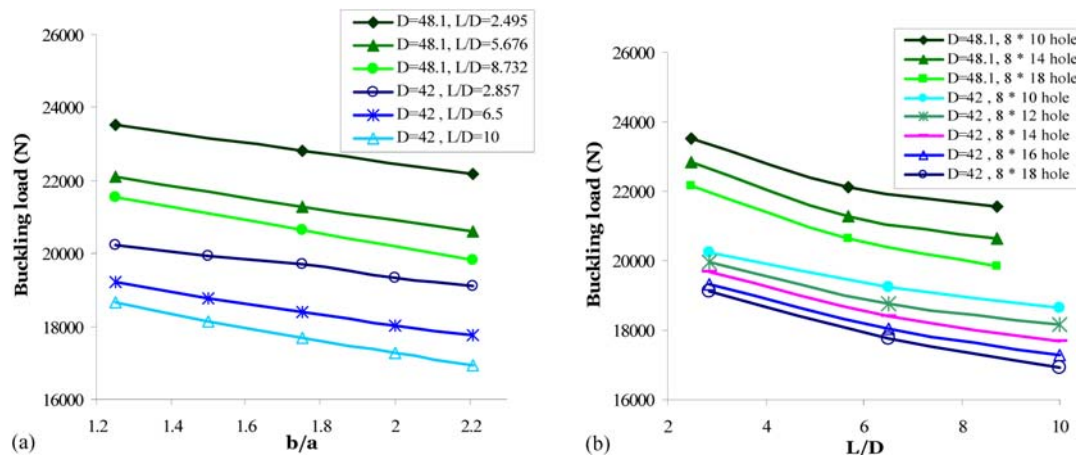


Figure 3. Summary of the buckling capacity of cylindrical shells versus (a) ratio b/a and (b) L/D for elliptical cutout with constant height and various widths.

3.1.2. Analysis of the effect of change in cutout width on the buckling load

In this section, the effect of changing the cutout width on the buckling load of cylindrical shells is studied. For this reason, cutouts with fixed height (8 mm) were created in the mid-height position of shells. Then, with changing the width of the cutouts from 10 to 18 mm, the change in buckling load was studied. The results of this analysis are presented in Table 3.

The buckling load vs. b/a and L/D ratios curves are

shown in Figs. 3a and 3b, respectively. The buckling load in these curves was not made dimensionless, so that we can compare the changes in the buckling load with the change in specimen diameter. The results show when the cutout height is constant, an increase in cutout width decreases the buckling load. It is evident from Fig. 3 that an increase in the cutout width when cutout height is constant causes a considerable reduction in the buckling load contrary to reverse state which had little effect on the buckling resistance of the shells.

Table 4. Summary of numerical analysis for cylindrical shells including an elliptical cutout with constant area

Model designation	Shell length (mm)	Cutout size (a×b)	Buckling Load (N)
D42-L420-L ₀ 210-8-17.7	420	8×17.7	16938.7
D42-L420-L ₀ 210-11-12.87	420	11×12.87	17798.7
D42-L420-L ₀ 210-14-10.11	420	14×10.11	18194.5
D42-L420-L ₀ 210-17.92-7.9	420	17.92×7.9	18513.6
D42-L273-L ₀ 136.5-8-17.68	273	8×17.68	17746.4
D42-L273-L ₀ 136.5-11-12.87	273	11×12.87	18419.9
D42-L273-L ₀ 136.5-14-10.11	273	14×10.11	18732.7
D42-L273-L ₀ 136.5-18.38-8	273	18.38×8	19027.9
D42-L120-L ₀ 60-8-17.6	120	8×17.6	19120.4
D42-L120-L ₀ 60-11-12.87	120	11×12.87	19713.9
D42-L120-L ₀ 60-14-10.11	120	14×10.11	20086.4
D42-L120-L ₀ 60-17.7-7.9	120	17.7×7.9	20293.5
D48.1-L420-L ₀ 210-7.94-17.54	420	7.94×17.54	19828.4
D48.1-L420-L ₀ 210-11-12.87	420	11×12.87	20656.5
D48.1-L420-L ₀ 210-14-10.11	420	14×10.11	20992.8
D48.1-L420-L ₀ 210-18-8	420	18×8	21431.2
D48.1-L273-L ₀ 136.5-8.02-17.86	273	8.02×17.86	20623.2
D48.1-L273-L ₀ 136.5-11-12.87	273	11×12.87	21222.3
D48.1-L273-L ₀ 136.5-14-10.11	273	14×10.11	21609.4
D48.1-L273-L ₀ 136.5-18-8	273	18×8	21838.7
D48.1-L120-L ₀ 60-8.04-17.75	120	8.04×17.75	22177.3
D48.1-L120-L ₀ 60-11-12.87	120	11×12.87	22661.1
D48.1-L120-L ₀ 60-14-10.11	120	14×10.11	23127.5
D48.1-L120-L ₀ 60-18-8	120	18×8	23318.7

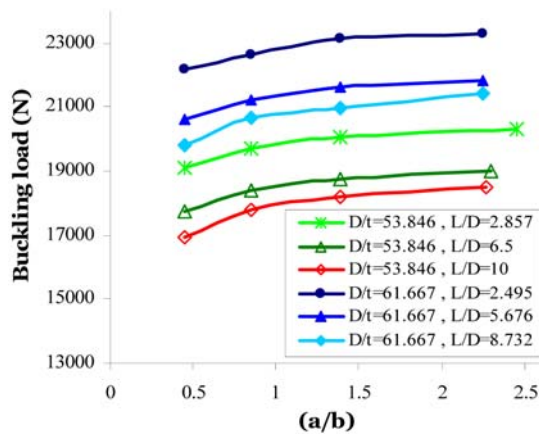


Figure 4. Plots of buckling load vs. ratio a/b for cylindrical shells include an elliptical cutout with constant area.

In cylindrical shells with a diameter of 42 mm, the change in the buckling load with the increase of cutout width from 10 to 18 mm was 9, 7.7, and 5.5%, for long, intermediate-length, and short shells, respectively.

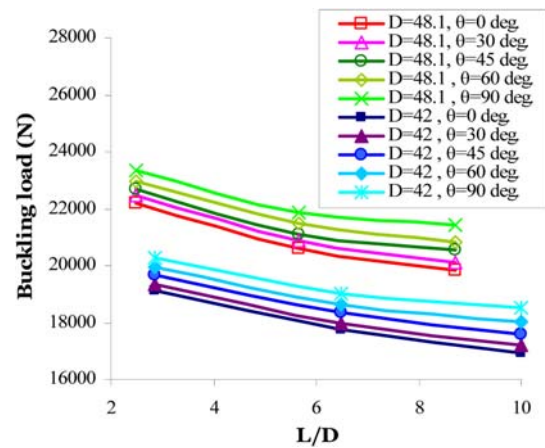


Figure 5. Plots of buckling load vs. ratio L/D for cylindrical shells including an elliptical cutout with constant dimensions and various angles.

In cylindrical shells with a diameter of 48.1 mm, with the increase of cutout width from 10 to 18 mm, the buckling load decreases 8, 6.7, and 5.7%, for long, intermediate-length, and short shells, respectively.

Table 5. Summary of numerical analysis for cylindrical shells including an elliptical cutout with various angles

Model designation	Shell length (mm)	Cutout angle (θ)	Buckling Load (N)
D42-L420-L ₀ 210-8-17.7	420	0	16938.7
D42-L420-L ₀ 210-8-18-30	420	30	17187.8
D42-L420-L ₀ 210-7.95-18-45	420	45	17611.8
D42-L420-L ₀ 210-8-18-60	420	60	18011.2
D42-L420-L ₀ 210-7.9-17.92-90	420	90	18513.6
D42-L273-L ₀ 136.5-8-17.68	273	0	17746.4
D42-L273-L ₀ 136.5-8-18-30	273	30	17986
D42-L273-L ₀ 136.5-7.98-17.68-45	273	45	18333
D42-L273-L ₀ 136.5-8-18-60	273	60	18634.4
D42-L273-L ₀ 136.5-8-18.38-90	273	90	19027.9
D42-L120-L ₀ 60-8-17.6	120	0	19120.4
D42-L120-L ₀ 60-8-17.7-30	120	30	19366
D42-L120-L ₀ 60-8-17.75-45	120	45	19654.2
D42-L120-L ₀ 60-8-17.7-60	120	60	19940.7
D42-L120-L ₀ 60-7.9-17.7-90	120	90	20293.5
D48.1-L420-L ₀ 210-7.94-17.54	420	0	19828.4
D48.1-L420-L ₀ 210-8-18-30	420	30	20094.2
D48.1-L420-L ₀ 210-7.96-17.66-45	420	45	20526.8
D48.1-L420-L ₀ 210-8-18-60	420	60	20823.2
D48.1-L420-L ₀ 210-8-18-90	420	90	21431.2
D48.1-L273-L ₀ 136.5-8.02-17.86	273	0	20623.2
D48.1-L273-L ₀ 136.5-8-18-30	273	30	20856.4
D48.1-L273-L ₀ 136.5-8-18-45	273	45	21096.7
D48.1-L273-L ₀ 136.5-8-18-60	273	60	21481.8
D48.1-L273-L ₀ 136.5-8-18-90	273	90	21838.7
D48.1-L120-L ₀ 60-8.04-17.75	120	0	22177.3
D48.1-L120-L ₀ 60-8-18-30	120	30	22467.4
D48.1-L120-L ₀ 60-8-17.75-45	120	45	22682
D48.1-L120-L ₀ 60-8-18-60	120	60	22932.7
D48.1-L120-L ₀ 60-8-18-90	120	90	23318.7

Table 6. Comparisons of the experimental and numerical results

Model designation	Buckling Load (N)		$\frac{ N_{EXP}-N_{FEM} }{N_{EXP}} \times 100\%$ error
	Experimental	Numerical	
D42-L420-perfect	23018.3	22792.8	0.99
D42-L420-L ₀ 210-8-17.7	16809.8	16938.7	0.77
D42-L420-L ₀ 210-12.05-17.95	16871.4	16540.1	1.96
D42-L420-L ₀ 210-14.05-17.95	16335.8	16500.2	1.01
D42-L420-L ₀ 210-8-9.98	18745	18654.3	0.48
D42-L420-L ₀ 210-8-14.05	17488.9	17691.1	1.16
D42-L273-perfect	22245.6	22814.8	2.5
D42-L273-L ₀ 136.5-8-17.68	17945.8	17746.4	1.11
D42-L273-L ₀ 136.5-12-17.8	17202.4	17459.7	1.5
D42-L273-L ₀ 136.5-14.08-18	17129	17332.2	1.19
D42-L273-L ₀ 136.5-8-9.95	18875.9	19224.3	1.85
D42-L273-L ₀ 136.5-7.96-13.84	18398.2	18406.7	0.05
D42-L120-perfect	23925.7	22751.6	5.1
D42-L120-L ₀ 60-8-17.6	20274.9	19120.4	5.69
D42-L120-L ₀ 60-12.1-18	18294.4	18782	2.67
D42-L120-L ₀ 60-14.05-18	17936.1	18772.1	4.66
D42-L120-L ₀ 60-8-10.88	19981.2	20241.7	1.3
D42-L120-L ₀ 60-8.27-14.07	18988.5	19691.7	3.7
D48.1-L420-perfect	25775.3	25876.9	0.4
D48.1-L420-L ₀ 210-7.94-17.54	19909.4	19828.4	0.4
D48.1-L420-L ₀ 210-7.95-9.88	22134.6	21550.2	2.64
D48.1-L420-L ₀ 210-7.96-13.84	20692.2	20644.5	0.23
D48.1-L273-perfect	26123.8	25858.7	1.0
D48.1-L273-L ₀ 136.5-8.02-17.86	20855.3	20623.2	1.11
D48.1-L273-L ₀ 136.5-8.02-9.92	23117.8	22104.3	4.38
D48.1-L273-L ₀ 136.5-8.02-13.92	21066.4	21293.2	1.08
D48.1-L120-perfect	26967.3	25825.4	4.4
D48.1-L120-L ₀ 60-8.04-17.75	21914	22177.3	1.2
D48.1-L120-L ₀ 60-8-9.9	23730.1	22824.9	3.81
D48.1-L120-L ₀ 60-8.04-13.85	22493.6	22177.3	1.4
D42-L420-L ₀ 210-7.95-18.45	17426.4	17611.8	1.06
D42-L420-L ₀ 210-7.9-17.92-90	18545.7	18513.6	0.17
D42-L273-L ₀ 136.5-7.98-17.68-45	17480.1	18333	4.87
D42-L273-L ₀ 136.5-8-18.38-90	18275.2	19027.9	4.11
D42-L120-L ₀ 60-8-17.75-45	20341.5	19654.2	3.37
D42-L120-L ₀ 60-7.9-17.7-90	20188.4	20293.5	0.52
D48.1-L420-L ₀ 210-7.96-17.66-45	20219.3	20526.8	1.52
D48.1-L120-L ₀ 60-8-17.75-45	21428.1	22682	5.85

it is evident that longer and slender shells are more sensitive to changes in cutout width.

Interestingly, when we compare these results with those presented in the previous section, we can see that when the height of the cutout is fixed and its width increases 8 mm, the amount of reduction in the buckling resistance is three times greater than the corresponding value in the state that the width of the cutout is fixed and its height increases 8 mm. Therefore, we recommend that in the design of these shells, whenever possible, the greater dimension of the cutout be oriented along the longitudinal axis of the cylinder.

3.1.3. Analysis of the effect of change in dimensions of fixed-area cutouts on the buckling behavior

In the previous sections, we studied the buckling behavior of the cylindrical shells by changing the height or width of the cutout, and in each case, the other dimension was kept constant. In this section, both width and height are changed, so that the product of height and width, which is representative of the cutout area, remains constant. Therefore, cutouts with an area of $A=111.2 \text{ mm}^2$ were created in the mid-height position of the shells. Four different values for cutouts height between 8 to 18 mm were considered; the corresponding values for the cutout

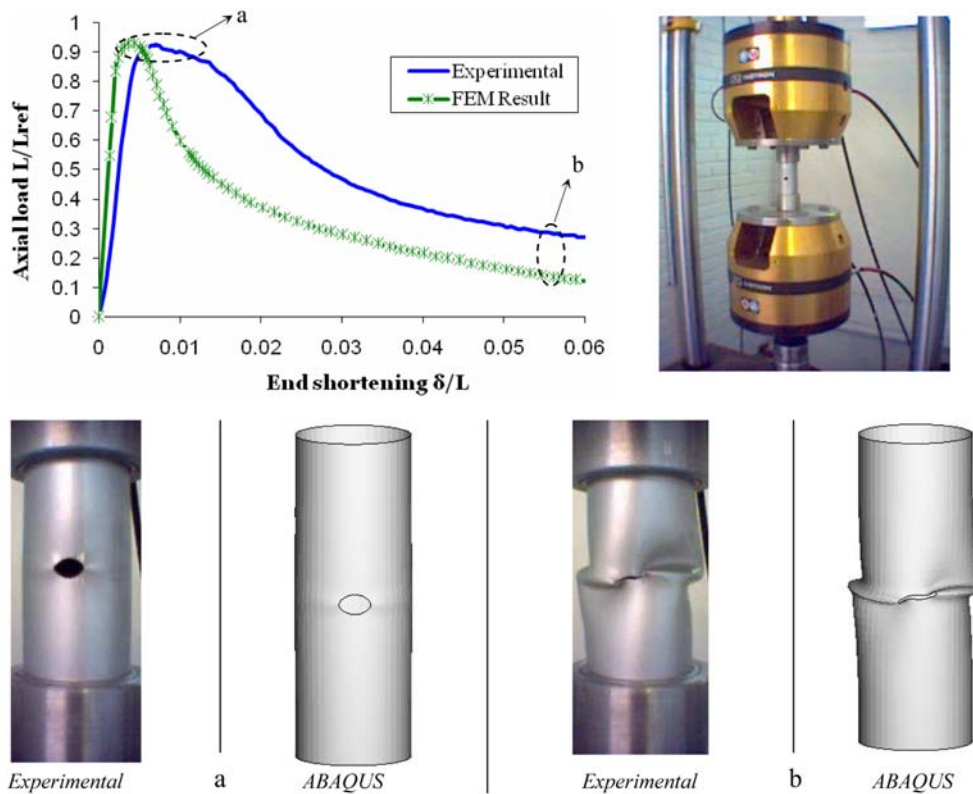


Figure 6. Comparison of the experimental and numerical results for the specimen D42-L120-L₀60-8-10.88.

width were calculated so that the cutout area was constant. Detailed information about the designed specimens and the analyses results are shown in Table 4. The curves of the buckling load versus the a/b ratio are shown in Fig. 4. As expected, Fig. 4 shows that the buckling load increases with increasing a/b ratio.

Figure 4 shows that shells with lower L/D and higher D/t ratio have a higher buckling load and they are more resistant to buckling. Furthermore, it is evident that buckling load is more sensitive to D/t ratio than L/D ratio.

3.2. Analysis of the effect of change in cutout angle on the buckling behavior of cylindrical Shells

In order to analyze the relationship between the buckling load and changes in the angle of elliptical cutouts, an elliptical cutout of fixed size (8×18 mm) was created in the mid-height position of cylindrical shells, with various angles between 0 and 90° . The results of this analysis are shown in Table 5.

The results show that increasing the cutout angle enhances the shell resistance against buckling and increases the amount of the critical load. Additionally, for long, intermediate-length, and short shells with a diameter of 48.1 mm, the buckling load increases 8, 6, and 5%, respectively. Therefore, longer and slender shells are more sensitive to the changes of the cutout angle.

The buckling load vs. L/D ratio curves are shown in Fig. 5. It can be seen that with an increase in the cutout angle, the buckling capacity of the shell increases. Also

for a cutout with fixed angle, the buckling load decreases with increasing L/D ratio.

4. Experimental VERification

Experimental tests using a servo hydraulic, INSTRON 8802 machine were conducted to verify some of the cases investigated in the numerical simulations.

The specimens were constrained by steel sleeve fixtures inserted at both ends, which mimics the fixed-fixed boundary condition used in the finite element simulations (see Fig. 6). Three specimens were tested for each case and almost identical results were obtained compared to those obtained from the numerical simulations.

The experimental results are compared to numerical findings in Table 6. The comparison shows that there is little difference between the two sets of data. It can be seen that the highest amount of discrepancy is related to short specimens (Shariati and Mahdizadeh 2008).

The mean difference between the numerical calculations and the experimental results is about 2% of experimental buckling load.

The load-end shortening curves and deformed shape of specimens in the buckling and post-buckling states in numerical and experimental tests are compared in Figs. 6 to 8. It can be seen that the slope of linear part of load-end shortening curves is higher in numerical analysis than in experimental results. This is maybe due to the presence of internal defects in the material which reduce the

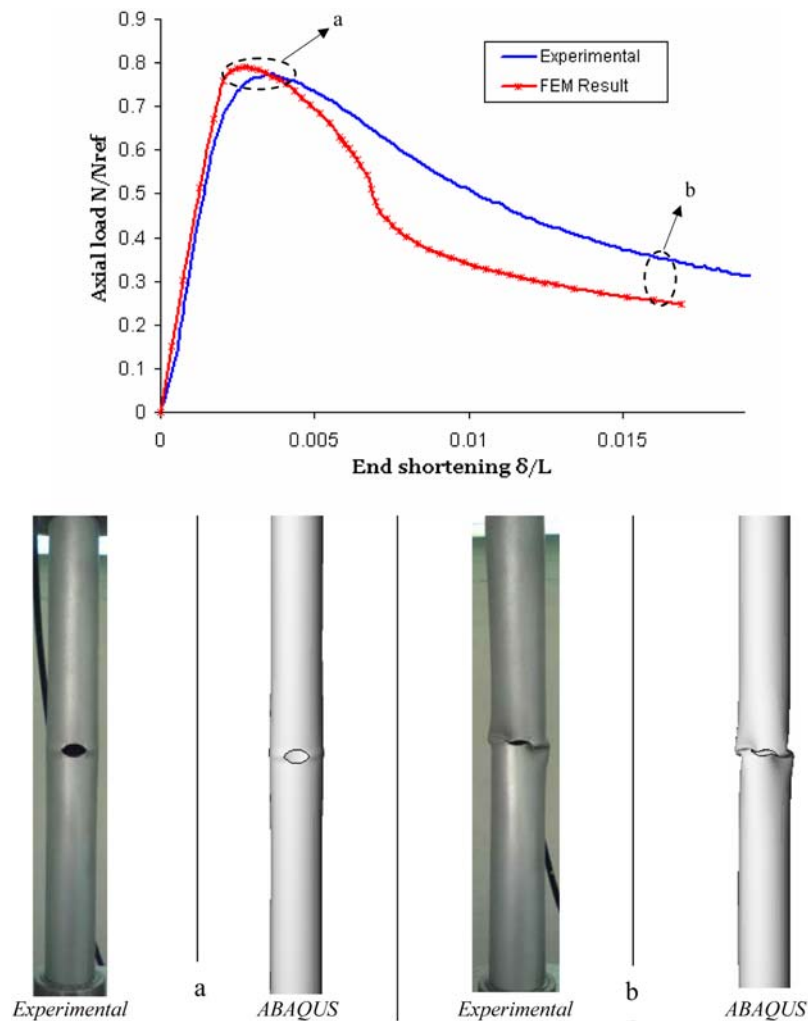


Figure 7. Comparison of the experimental and numerical results for the specimen D42-L420-L₀210-12.05-17.95.

stiffness of the specimens in the experimental method, while the materials are assumed to be ideal in the numerical analyses.

Comparison of deformations resulted by numerical and experimental methods for the specimens shown in Figs. 6 to 8 in the buckling and post-buckling states, shows that almost identical results were obtained.

5. Empirical-Numerical Equations

Based on the numerical and experimental dimensionless buckling loads of shells, formulas are presented here using Lagrangian polynomial for the computation of the buckling load of cylindrical shells with elliptical cutouts subject to axial compression. To get these formulas, surfaces were fitted to the dimensionless buckling load values using Lagrangian polynomial method (Gerald, 1999). K_{cutout} is introduced as a buckling load reduction factor for cylindrical shells with cutout (dimensionless buckling load) and defined according to eq. (3).

$$K_{cutout} = \frac{N_{cutout}}{N_{perfect}} \tag{3}$$

Where $N_{perfect}$ is the buckling load for perfect cylindrical shells per unit perimeter of cylindrical shell's cross section, and N_{cutout} and K_{cutout} are the buckling load per unit perimeter of cylindrical shell's cross section, and dimensionless buckling load, for cylindrical shells with cutout. The general form of K_{cutout} is according to eq. (4).

$$K_{cutout}(\alpha, \beta, \gamma, \eta, \theta) = A + B\alpha + C\alpha^2 + D\beta + E\beta^2 + F\gamma + G\gamma^2 + H\alpha\gamma + I\beta\gamma + J\lambda\gamma + K\theta + L\theta^2 + M\eta + N\eta^2 + \dots \tag{4}$$

Where $\alpha = a/D$, $\beta = b/D$, $\gamma = L/D$, $\eta = a/b$ and θ is the cutout angle in radian. The coefficients A, B, C, ... are computed using Lagrangian polynomial method.

The exact form of the resulting equations is summarized in Table 7. Both experimental and numerical results (in situations that experimental data were not available) are used in these equations.

Eq. (5) is the reduction factor for the cylindrical shells

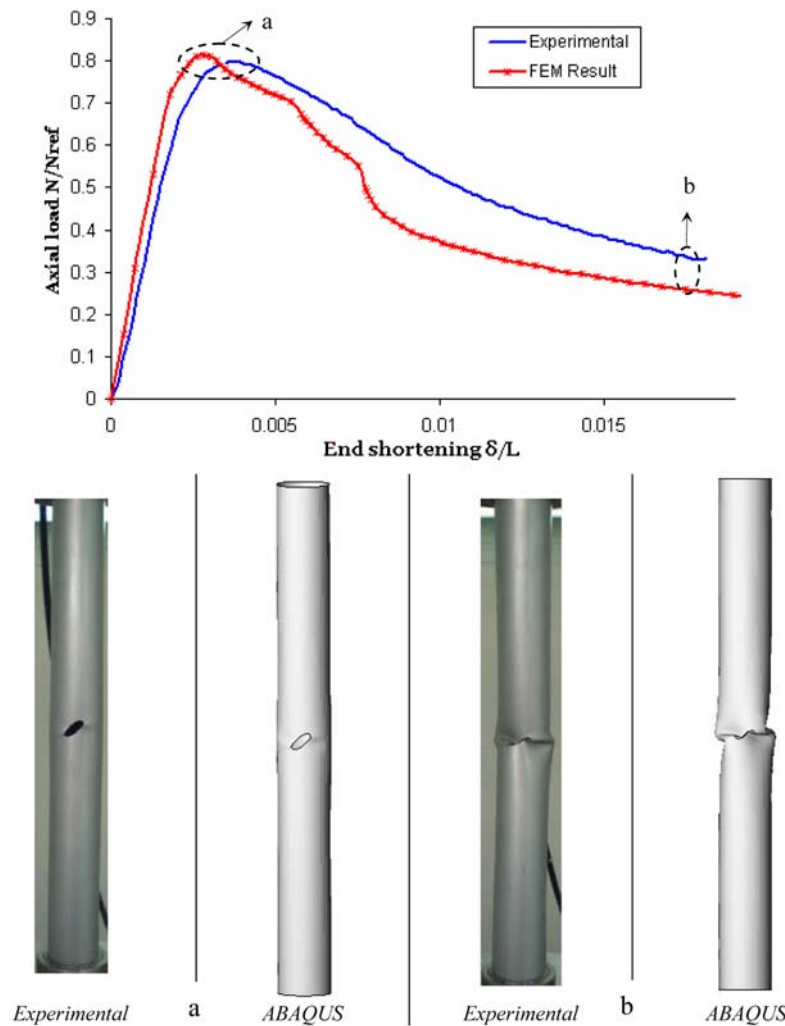


Figure 8. Comparison of the experimental and numerical results for the specimen D42-L420-L0210-7.95-18-45.

with the ratio $D/t=53.846$ and various lengths ($2.857 \leq L/D \leq 10$), with an elliptical cutout of fixed width ($b/D=0.4286$) and various heights ($0.1905 \leq a/D \leq 0.3333$) in the mid-height position of the shell.

Eq. (6) is the reduction factor for the cylindrical shells with the ratio $D/t=53.846$ and various lengths ($2.857 \leq L/D \leq 10$), with an elliptical cutout of fixed height ($a/D=0.1905$) and various widths ($0.2381 \leq b/D \leq 0.428$) in the mid-height position of the shell.

Eq. (7) is the reduction factor for the cylindrical shells with the ratio $D/t=53.846$ and various lengths ($2.857 \leq L/D \leq 10$), with an elliptical cutout of fixed size $8 \times 18 \text{ mm}^2$ and various angles ($0^\circ \leq \theta \leq 90^\circ$) in the mid-height position of the shell.

Eq. (8) is the reduction factor for the cylindrical shells with the ratio $D/t=53.846$ and various lengths ($2.857 \leq L/D \leq 10$), with an elliptical cutout of fixed area $A'=111.2 \text{ mm}^2$ and various dimensions ($0.444 \leq a/b \leq 2.25$) in the mid-height position of the shell.

Eq. (9) is the reduction factor for the cylindrical shells with the ratio $D/t=61.667$ and various lengths ($2.4948 \leq L/D \leq 8.732$), with an elliptical cutout of fixed width (b/D

$=0.3742$) and various heights ($0.1663 \leq a/D \leq 0.291$) in the mid-height position of the shell.

Eq. (10) is the reduction factor for the cylindrical shells with the ratio $D/t=61.667$ and various lengths ($2.4948 \leq L/D \leq 8.732$), with an elliptical cutout of fixed height ($a/D=0.1663$) and various widths ($0.2079 \leq b/D \leq 0.374$) in the mid-height position of the shell.

Eq. (11) is the reduction factor for the cylindrical shells with the ratio $D/t=61.667$ and various lengths ($2.4948 \leq L/D \leq 8.732$), with an elliptical cutout of fixed size $8 \times 18 \text{ mm}$ and various angles ($0^\circ \leq \theta \leq 90^\circ$) in the mid-height position of the shell.

Eq. (12) is the reduction factor for the cylindrical shells with the ratio $D/t=61.667$ and various lengths ($2.4948 \leq L/D \leq 8.732$), with an elliptical cutout of fixed area $A'=111.2 \text{ mm}^2$ and various dimensions ($0.444 \leq a/b \leq 2.25$) in the mid-height position of the shell.

6. Concluding Remarks

The paper examines the influence of elliptical cutouts of various sizes and angles on the nonlinear response of

Table 7. The empirical equations for predicting the buckling load reduction factors of cylindrical shells

Equation No.	Parameters	Empirical equations
(5)	γ, α	$K_{cutout}=0.015\gamma-0.00876\gamma^2-0.15019\gamma^2\alpha^2+0.0668\gamma^2\alpha+0.8802\gamma\alpha^2-2323\gamma\alpha-2.601\alpha+1.2529+2.597\alpha^2$
(6)	γ, β	$K_{cutout}=-8.997\beta+0.0233\gamma^2+0.2518\gamma^2\beta^2-0.1658\gamma^2\beta-3.7786\gamma\beta^2+2.4219\gamma\beta-0.3411\gamma+13.984\beta^2+2.1389$
(7)	γ, θ	$K_{cutout}=0.8516-0.07677\gamma\theta+0.00609\gamma^2\theta-0.1084\theta^2+0.1790-0.00318\gamma^2\theta^2-0.00149\alpha^2+0.0444\gamma\theta^2+0.0028\gamma$
(8)	γ, η	$K_{cutout}=-0.1163\beta^3-0.75229\eta^2+0.000775\gamma^2+0.17221\gamma\eta+0.0208\gamma\eta^3-0.11429\gamma\eta^2-0.000539\gamma^2\eta^3+0.00409\gamma^2\eta^2-0.00676\gamma^2\eta+1.0896+0.5519\eta^2-0.0536\gamma$
(9)	γ, α	$K_{cutout}=0.10969\gamma-0.1375\gamma^2\alpha^2+0.073\gamma^2\alpha+1.77\gamma\alpha^2-0.9494\gamma\alpha+0.56938-0.00898\gamma^2-4.1643\alpha^2+2.1681\alpha$
(10)	γ, β	$K_{cutout}=+3.052\beta-0.0292\gamma^2-0.3382\gamma^2\beta^2+0.2028\gamma^2\beta+3.8113\gamma\beta^2-2.3034\gamma\beta+0.329\gamma-5.639\beta^2+0.4622$
(11)	γ, θ	$K_{cutout}=0.16479\theta^2-0.20166\theta+0.00349\gamma^2\theta^2-0.000639\gamma^2-0.04609\gamma\theta^2+0.00727\gamma+0.81477-0.0043\gamma^2\theta+0.05989\gamma\theta$
(12)	γ, η	$K_{cutout}=0.0229\gamma+0.75717+0.002277\gamma^2\eta^2-0.010069\gamma^2\eta^2+0.01396\gamma^2\eta-0.023389\gamma\eta^3+0.1055\gamma\eta^2-0.1497\gamma\eta-0.003289\gamma^2+0.4384\eta-0.274178\eta^2+0.05646\eta^3$

steel cylindrical shells subjected to axial compression. To that end, shells with various L/D and D/t ratios were considered. The influence of the size and angle of cutouts at the mid length of the shells was also investigated. Very good correlation was observed between the results of the experimental and numerical simulations. In addition, the following results were found:

When the cutout width is constant and height of the cutout increases, the buckling load reduces. However, the amount of reduction in the buckling load is negligible. Increasing the width of the cutout while the cutout height is constant decreases the buckling load extremely. Therefore, it is preferable to design the shells in such a way that the greater dimension of the cutout is aligned with the longitudinal axis of the shell.

The buckling load increases with increasing the height-to-width ratio of cutout in cylindrical shells with a cutout of fixed area. Also, increasing the cutout angle enhances the shell resistance and increases the buckling load.

Finally, formulas were presented for the computation of the buckling load of cylindrical shells with elliptical cutouts based on the buckling load of perfect cylindrical shells. These relationships are applicable to a wide range of cylindrical shells with elliptical cutouts.

7. References

- Almorth, B. O., Brogan F. A., and Marlowe, M. B. (1973). "Stability analysis of cylinders with circular cutouts." *American Institute of Aeronautics and Astronautics Journals*, 11(11), pp. 1582-1584.
- Amazigo, J. C. and Budiansky, B. (1972). "Asymptotic formulas for the buckling stress of axially compressed cylinders with localized or random axisymmetric imperfections." *Journal of Applied Mechanics*, 39, pp. 179-184.
- Arbocz, J. and Ho, J. M. A. M. (1991). "Collapse of axially compressed cylindrical shells with random imperfections." *American Institute of Aeronautics and Astronautics Journals*, 29, pp. 2247-2256.
- ASTM (2005). *ASTM A 370-05*. Standard Test Methods and Definitions for Mechanical Testing of Steel Products, USA, pp. 2-5.
- Blachut, J. (2010). "Buckling of axially compressed cylinders with imperfect length." *Computers & Structures*, 88(5-6), pp. 365-374.
- Camotim, D., Silvestre N., and Dinis, P. B. (2005). "Numerical Analysis of Cold-Formed Steel Members." *International Journal of Steel Structures*, 5(1), pp. 63-78.
- Gerald, C. F. and Wheatley, P. O. (1999). *Applied Numerical Analysis*. Addison Wesley, New York, USA.
- Han, H., Cheng, J., and Taheri, F. (2006). "Numerical and experimental investigations of the response of aluminum cylinders with a cutout subject to axial compression." *Thin-Walled Structures*, 44, pp. 254-270.
- Jullien, J. F. and Limam, A. (1998). "Effect of openings on the buckling of cylindrical shells subjected to axial compression." *Thin-Walled Structures*, 31, pp. 187-202.
- Krishnakumar, S. and Forster, C. G. (1991). "Axial load compatibility of cylindrical shells with local geometric defects." *Experimental Mechanics*, 31, pp. 104-110.
- Kuwamura, H. (2003). "Local Buckling of Thin-Walled Stainless Steel Members." *International Journal of Steel Structures*, 3(3), pp. 191-201.
- Lee, J., Nguyen, H. T., and Kim, S. E. (2009). "Buckling and Post Buckling of Thin-walled Composite Columns with Intermediate-stiffened Open Cross-section under Axial Compression." *International Journal of Steel Structures*, 9(3), pp. 175-184.
- Lim, C. W., Ma, Y. F., Kitipornchai, S., Wang, C. M., and Yuen, R. K. K. (2003). "Buckling of vertical cylindrical shells under combined end pressure and body force." *ASCE J. Eng. Mech.*, 129(8), pp. 876-884.

- Nadia, B., Gabriele, E., and Riccardo, Z. (2005). "Buckling Design Analysis of Thin-walled Compressed Members with or without Perforations." *International Journal of Steel Structures*, 5(1), pp. 33-42.
- Pircher, M. and Bridge, R. Q. (2001). "The influence of circumferential weld-induced imperfections on the buckling of silos and tanks." *Journal of Constructional Steel Research*, 57, pp. 569-580.
- Pircher, M., Berry, P. A., Ding, X. L., and Bridge, R. Q. (2001). "The shape of circumferential weld induced imperfections in thin walled steel silos and tanks." *Thin-Walled Structures*, 39(12), pp. 999-1014.
- Poursaeidi, E., Rahimi, G. H., and Vafai, A. H. (2004). "Plastic buckling of cylindrical shells with cutouts." *Asian Journal of civil engineering (Building and housing)*, 5(3-4), pp. 191-207.
- Prabu, B., Raviprakash, A. V., and Venkatraman, A. (2010). "Parametric study on buckling behaviour of dented short carbon steel cylindrical shell subjected to uniform axial compression." *Thin-Walled Structures*, 48(8), pp. 639-649.
- Rasmussen, K. J. R., Burns, T., Bezkorovainy, P., and Bambach, M. R. (2005). "Recent Research on the Local Buckling of Cold-formed Stainless Steel Sections." *International Journal of Steel Structures*, 5(1), pp. 87-100.
- Schenk, C. A. and Schuëller, G. I. (2007). "Buckling analysis of cylindrical shells with cutouts including random boundary and geometric imperfections." *Computer Methods in Applied Mechanics and Engineering*, 196(35-36), pp. 3424-3434.
- Schneider, W. (2006). "Stimulating equivalent geometrical imperfections for the numerical buckling strength verification of axially compressed cylindrical steel shells." *Computational Mechanics*, 37(6), pp. 530-536.
- Shariati, M. and Mahdizadeh Rokhi, M. (2008). "Numerical and Experimental Investigations on Buckling of Steel Cylindrical Shells with Elliptical Cutout Subject to Axial Compression." *Thin-Walled Structures*, 46, pp. 1251-1261.
- Shariati, M. and Mahdizadeh Rokhi, M. (2009). "Investigation of buckling of Steel cylindrical shells with elliptical cutout under bending moment." *International Review of Mechanical Engineering*, 3(1), pp. 7-15.
- Starnes, Jr. J. H. (1974). "The effects of cutouts on the buckling of thin shells." In: Fung YC, Sechler EE, editors. *Thin-shell structures*. Englewood Cliffs, Prentice-Hall, NJ, pp. 289-304.
- Tafreshi, A. (2002). "Buckling and post buckling analysis of composite cylindrical shells with cutout subjected to internal pressure and axial compression load." *Int. J. Pressure Vessel Piping*, 79, pp. 351-359.
- Tafreshi, A. and Colin, G. B. (2006). "Instability of imperfect composite cylindrical shells under combined loading." *Composite Structure*, 80(1), pp. 49-64.
- Timoshenko, S. P. and Gere, J. M. (1961). *Theory of elastic stability. 2nd, Edition*, McGraw-Hill Book Co., Inc., New York, N.Y., USA.
- Toda, S. (1983). "Buckling of cylinders with cutouts under axial compression." *Exp. Mech.*, 23(4), pp. 414-417.
- Vartdal, B. J., Al-Hassani, S. T. S., and Burley, S. J. (2005). "A tube with a rectangular cutout. Part 2: subject to axial compression." *Proc. IMechE, 220 Part C: J. Mechanical Engineering Science*, 220(5), pp. 652-643.
- Yeh, M. K., Lin, M. C., and Wu, W. T. (1999). "Bending buckling of an elastoplastic cylindrical shell with a cutout." *Engineering Structures*, 21, pp. 996-1005.